

KFKI-1987-81/6

J. DOORENBOS  
A. GACS  
ZS. KISS

SIMULATION OF THE DYNAMIC BEHAVIOUR  
OF THE SECONDARY CIRCUIT OF A WWER-440  
TYPE NUCLEAR POWER PLANT

PART 2

*Hungarian Academy of Sciences*

**CENTRAL  
RESEARCH  
INSTITUTE FOR  
PHYSICS**

**BUDAPEST**

SIMULATION OF THE DYNAMIC BEHAVIOUR  
OF THE SECONDARY CIRCUIT OF A WWR-440  
TYPE NUCLEAR POWER PLANT

PART 2

J. DOORENBOS\*, A. GÁCS, ZS. KISS

Central Research Institute for Physics  
H-1525 Budapest 114, P.O.B. 49, Hungary

\*Iowa State University

J. Doorenbos, A. Gács, Zs. Kiss: Simulation of the dynamic behaviour of the secondary circuit of a WWER-440 type Nuclear Power Plant. Part 2. KFKI-1987-81/G

#### ABSTRACT

This report describes the dynamic simulation models of the most important controllers of the secondary circuit of a WWER-440 type Nuclear Power Plant i.e. the hydraulic turbine controller and the level controls of the condenser hotwell and that of the feedwater tank. Simulation results are also presented. This paper continues the descriptions of the dynamic simulation models of the primary circuit (Reports KFKI-1983-127 and KFKI-1985-08), and the secondary circuit (Report KFKI-1987-44/G) of this type nuclear power plants.

Я. Дооренбос, А. Гач, Ж. Киш: Симуляция динамики второго контура АЭС типа ВВЭР-440. Часть 2. КФКИ-1987-81/Г

#### АННОТАЦИЯ

В отчете описана модель, которая служит для симуляции динамики второго контура АЭС с реакторами типа ВВЭР-440. Задачей модели является моделирование нестационарных процессов в номинальных режимах и при небольших авариях в принципиальном симуляторе. Данная работа - продолжение отчетов КФКИ-1983-127 и КФКИ-1985-08, в которых описывается модель первого контура АЭС с реакторами типа ВВЭР-440. Актуальное состояние модели не содержит регулирующие органы второго контура. В отчете даются некоторые симуляционные результаты.

Doorenbos J., Gács A., Kiss Zs.: WWER-440 típusu atomerőmű szekunderköre dinamikus tulajdonságainak szimulációja. II. rész. KFKI-1987-81/G

#### KIVONAT

Ez a riport egy VVER-440 típusu atomerőmű szekunderköre legfontosabb szabályozóinak dinamikus szimulációs modelljét írja le, így a hidraulikus turbínaszabályozást valamint a kondenzátorzsomp és a tápviztartály vízszint-szabályozóit. Szimulációs eredményeket is bemutatunk. Ez a dolgozat folytatása az ilyen típusu atomerőművek dinamikus szimulációs modelljeit leíró riportjainak (példakör: KFKI-1983-127 és KFKI-1985-08; szekunderkör: KFKI-1987-44/G).

## 1. INTRODUCTION

A basic principles simulator is under construction in our Institute for WWER-440 type Nuclear Power Plants. The purpose of this simulator is to provide a means of studying the normal and close-to-normal operating states of WWER-440 power plants and to help in teaching the essential control concepts of these units.

The first part of this report /KFKI-1987-44/G/ has already been published and it describes the models of the main technological units of the secondary circuit. The scope of simulation is now extended to the most important controllers of the secondary circuit; the models of these controllers are described in the present paper. The controllers to be discussed are the following:

- the hydraulic turbine controller,
- the level control of the condenser hotwell,
- the level control of the feedwater tank.

## 2. THE HYDRAULIC TURBINE CONTROLLER

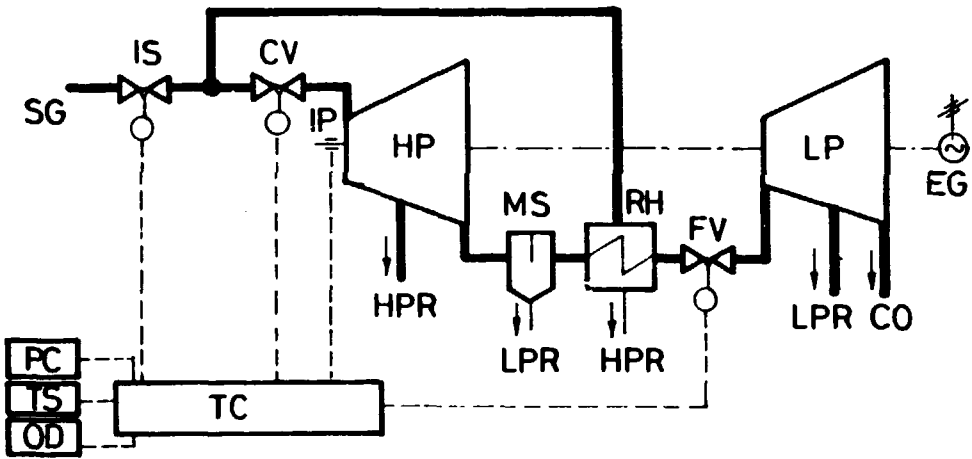
The steam turbine model is discussed in Part 1 of this report. The high pressure and the low pressure turbines are connected through a moisture separator and reheater unit. The inlet flows of both turbines are to be controlled.

The principle of nozzle control is well-known: various arrangements of valves are employed as automatic devices. Due to the large output and the high-pressure steam, a hydraulic controller unit is also needed for the steam valves of the K-220-44 type turbines used in WWER-440 type power plants.

As a means of simplifying our approach, we can divide the steam valves into groups, viz.

- isolation valves /to prevent admission of steam to both the turbine and the heating side of the reheater unit in the case of rapid transients/,
- main steam control valves /to set the inlet steam pressure of the high pressure turbine according to the load to be followed/,
- flap valves /to provide protection for the low pressure turbine during transients/.

Each of these groups can be simulated by a single valve model, i.e. one isolation valve /IS/, one control valve /CV/, and one flap valve /FV/, as shown in Fig.1.



TC hydraulic turbine controller  
PC inputs from power control unit /setpoint/  
TS " " techn. signals /protections, etc./  
OD " " operator's desk /inhibitions, etc./  
SG main steam from steam generators  
IS isolation valve  
CV control valve  
IP impeller /turbine speed/  
HP high pressure turbine  
HPR to high pressure reheat of feedwater  
MS moisture separator  
RH reheat of working steam  
FV flap valve  
LP low pressure turbine  
LPR to low pressure reheat of condensate  
CO exhaust to main steam condenser  
EG electrical generator

Fig.1 Stear valves and control

The modelling of the hydraulic turbine controller is necessary to accurately simulate normal transients that occur during the operation of the turbine. The controller has a great influence during transients such as load change and transition to the no-load state. The controller is also the only connection to the isolation valves, the control valves, and the flap valves. All control functions must be effected through the use of the hydraulic controller unit.

### 2.1. Controller Operation

A simplified diagram of the controller showing the most important functional blocks is given in Figure 2. The basic principles of operation of each of the blocks are important for simulation purposes, but the exact details are unimportant and unnecessary.

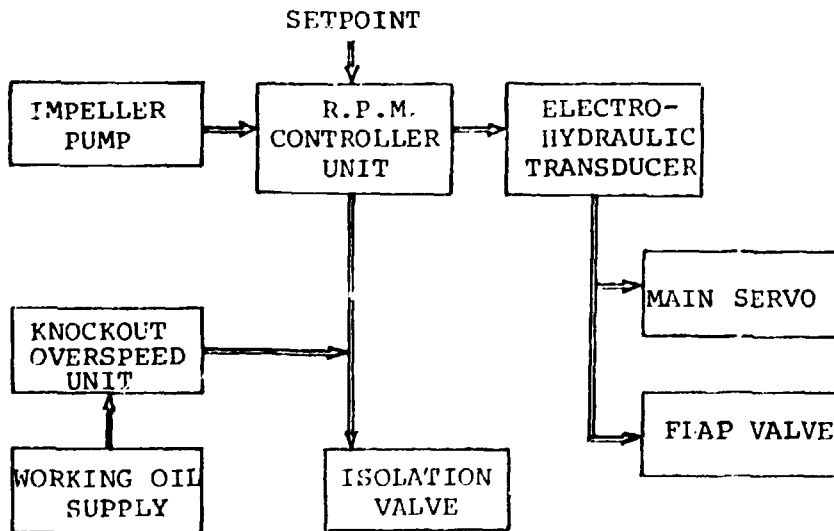


Fig.2 Simplified Controller Diagram

The steam valves are held open by oil pressure against springs that close the valves when the oil pressure is decreased or lost. The valve positions are varied by varying the controlling oil pressures.

The isolation valves are held open by the working oil pressure. The working oil is supplied at a constant pressure of approximately 16.5 bar. This pressure holds the isolation valves in their fully opened state during normal operation.

Both the control valves and the flap valves are controlled by the control oil pressure. The control valves are controlled indirectly by a servomotor. The control oil pressure is determined by the R.P.M. controller unit. This control oil pressure being derived from the working oil pressure by means of a variable gap that allows some of the control oil to flow out. The working oil enters through a fixed gap and exits through a variable gap. This is illustrated in Figure 3. The control oil flows out through the variable gap to atmospheric pressure of approximately 1 bar. The control oil pressure ranges from approximately 1.2 bar when the variable gap is fully open to the working oil pressure of 16.5 bar when the gap is completely closed.

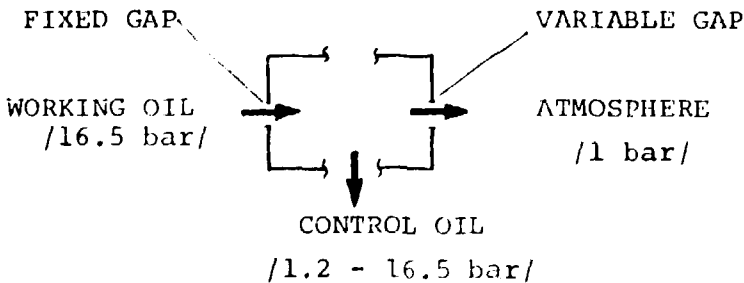


Fig.3 Determination of Control Oil Pressure



The size of the variable gap is determined by the relative positions of the setpoint sleeve and the impeller piston. The setpoint sleeve is connected to the setpoint unit so that an increase in the setpoint causes the gap size to decrease and the control oil pressure to increase; this opens the control valves. A decrease in the setpoint increases the gap size, decreases the control oil pressure, and closes the control valves.

The impeller piston position is determined by the impeller oil pressure. An impeller pump is connected to the axis of the turbine. The pressure of the oil from the impeller pump is proportional to the rotational speed of the turbine. This oil pressure moves the impeller piston inside the setpoint sleeve so that an increase in rotational speed causes an increase in impeller oil pressure which causes the gap to open. The opening of the gap lowers the control oil pressure and closes the control valves until a new equilibrium point is established.

An electro-hydraulic transducer unit has also been installed on the controller. Under normal conditions, it does not affect the operation of the turbine. In the case of a loss of load, however, the electro-hydraulic transducer plays an important role in the control of the turbine. The electro-hydraulic transducer provides a quick response to a trip of the generator breakers. When the breakers are tripped, a current function is generated that causes the electro-hydraulic transducer to allow some of the control oil to flow out. This flow of control oil lowers the control oil pressure and closes the control valves. The control oil flow is proportional to the current. Without this quick response, the turbine would trip because of an overspeed condition before reaching its no-load state because the response time of the rest of the controller is too slow.

The overspeed protection /OP/ and the knockout magnet /KM/ close all three types of valves. The OP and the KM operate in the same way: the working oil is allowed to flow out and the working oil pressure drops thereby causing the isolation valves to close. This drop in working oil pressure also causes the control oil pressure to drop and the control and flap valves to close.

## 2.2. Modelling the Controller

Although the actual controller is quite complex, it can be simplified and broken down into several block operations for simulation. The following six blocks were chosen for the simulation:

1. Calculation of a pseudo servo position from turbine speed and the setpoint
2. Calculation of a multiplier to simulate the electro-hydraulic transducer.
3. Calculation of the position of the isolation valve.
4. Calculation of a corrected pseudo servo position.
5. Calculation of the control valve position and the effective cross sectional area.
6. Calculation of the flap valve position.

A block diagram of the necessary inputs, calculations, and outputs is given in Figure 4.

First the size of the gap is determined. The impeller piston position is determined by a linear relationship from the turbine rotational speed, bypassing the calculation of the impeller oil pressure. The setpoint sleeve position is determined by a linear relationship from the setpoint input. These two positions are then subtracted to determine the size of the gap.

In the actual controller, the control oil pressure is determined by the gap size, This relationship is quite non-linear.

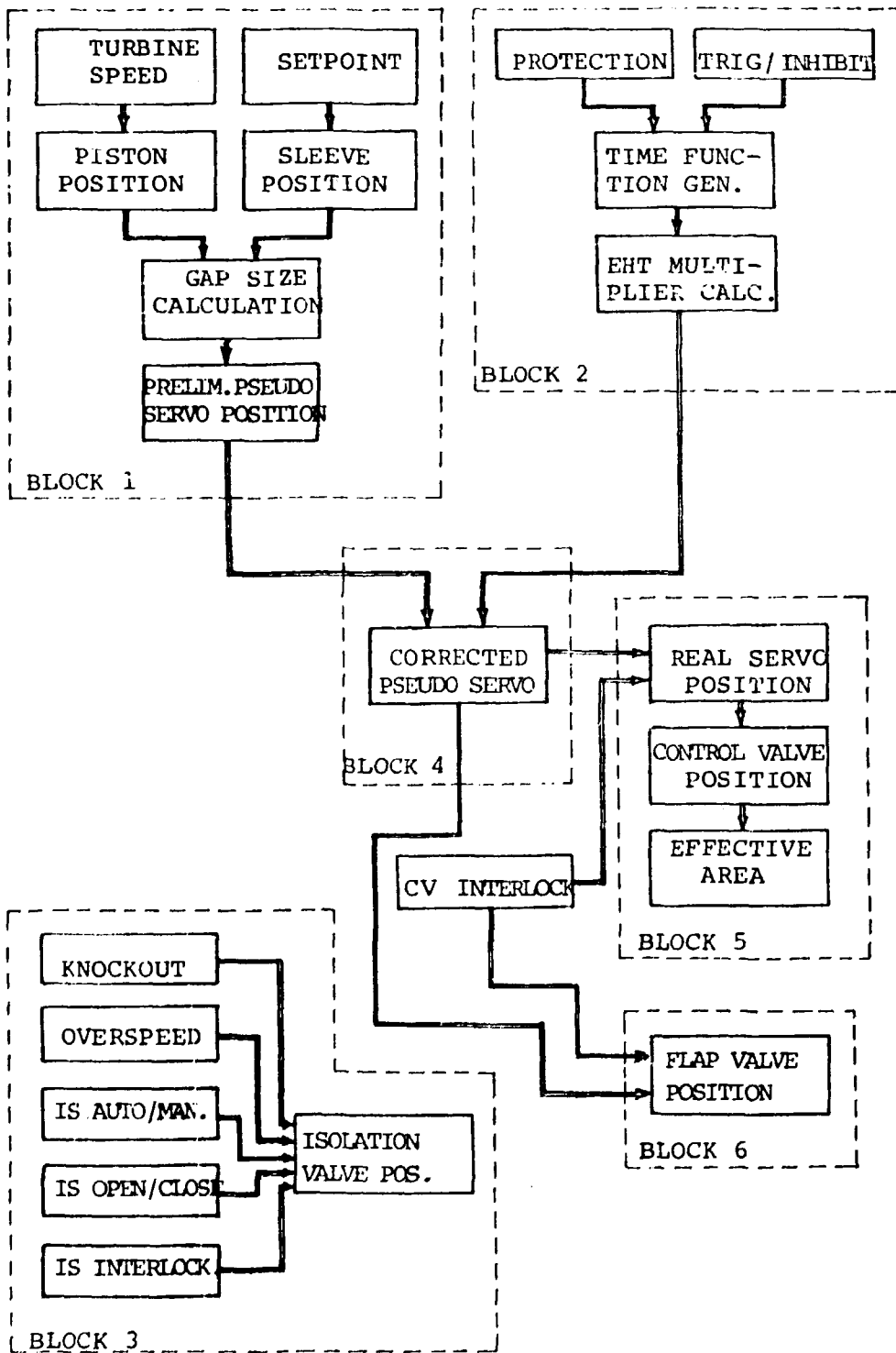


Fig. 4 Block Diagram of Controller Model

The relationship between the control oil pressure and the main servo position is also quite non-linear. However, the relationship between the gap size and the main servo position is nearly linear so that a linear approximation may be used. This also eliminates the unnecessary intermediate calculation of the control oil pressure. Since the control oil pressure is not displayed on the basic principles simulator, its calculation is not required.

There is one minor problem with this approach, though. The main servo position ranges from  $\emptyset$  to 32 $\emptyset$  mm over a control oil pressure range of 4.2 to 1 $\emptyset$ .5 bar. This is less than the actual control oil pressure range of 1.2 to 16.5 bar as is shown in Figure 5. To solve this problem, a pseudo servo position is calculated instead. This pseudo servo position ranges from  $\emptyset$  to 783 mm to cover the entire control oil pressure range. The real main servo position can be determined by subtracting 3 $\emptyset$ 8 from the pseudo servo position. This offset of 3 $\emptyset$ 8 mm corresponds to a control oil pressure of 4.2 bar, the zero point of the real servo position. After the subtraction, the result is limited so that it is between  $\emptyset$  and 32 $\emptyset$ mm.

The next step in the simulation process is to simulate the effect of the electro-hydraulic transducer. As mentioned earlier, the electro-hydraulic transducer only affects the operation of the controller in the case of a protection. This protection initiates a current time function to activate the electro-hydraulic transducer. The state of the protection input is checked. If the protection is activated, and it is not inhibited, the current function is initiated. This current function is simulated by a piece-wise linear function. The current applied to the electro-hydraulic transducer is then converted to a multiplier scaled from  $\emptyset$ . $\emptyset$  to 1. $\emptyset$  from another piece-wise linear function. This multiplier will be multiplied by the pseudo servo position to obtain a corrected pseudo servo position and to simulate the decrease in control oil pressure.

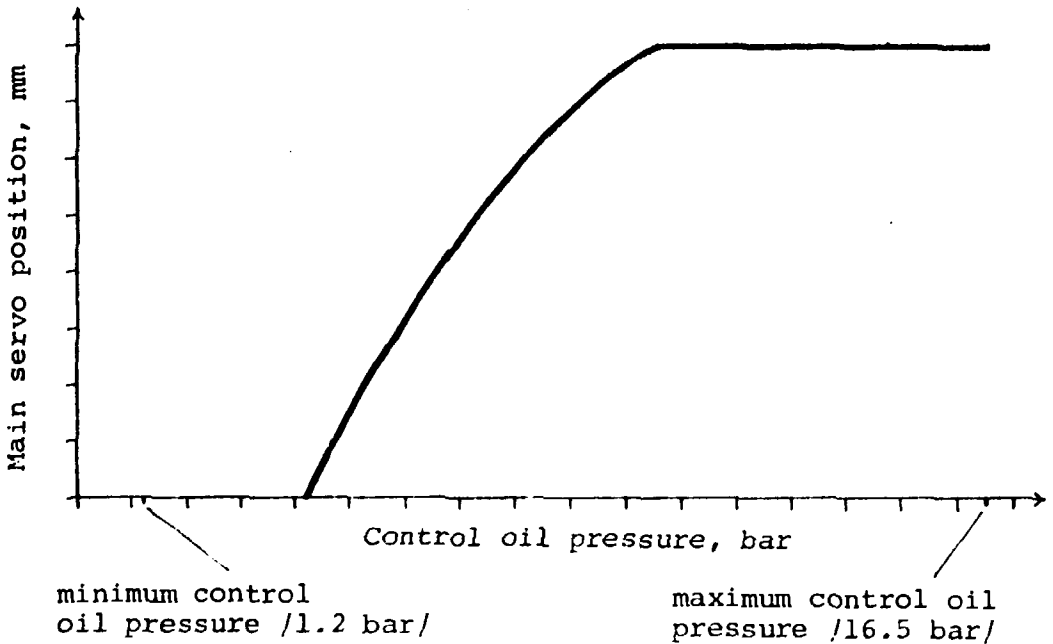


Fig.5 Main Servo Position versus Control Oil Pressure

Next, the position of the isolation valves is determined. For simulation purposes, the isolation valves are replaced by a single valve. The same is true for the control valves and flap valves. The positions are calculated as a fraction of completely open state; thus, their values are between 0.0 and 1.0. If a knockout or overspeed condition is active, the isolation valve position is set immediately to zero since its closing time of 0.45 s is much less than the simulation step size of 1.0 s. If the rotational speed of the turbine is below a certain level, a second press of the knockout switch allows a knockout state to be deactivated.

The simulator also allows for the manual control of the isolation valve. If the isolation valve is under automatic con-

trol, it will be fully open unless an overspeed or knockout condition is active. In that case, it will be completely closed.

In manual mode, it is possible to open and close the valve in steps by issuing open and close commands.

The interlock signal from the plant logics is also simulated. This signal prohibits the opening of the isolation valve until the interlock signal returns to its inactive state.

After calculating the isolation valve position, the corrected pseudo servo position is calculated. This is done based on the preliminary pseudo servo position and the state of the knock-out and overspeed protections. If either an overspeed or a knockout is active, the pseudo servo position is set to zero because the working oil pressure is lost, and the control oil pressure is at its minimum value. Otherwise, the preliminary pseudo servo position is multiplied by the multiplier that was determined earlier.

The corrected pseudo servo position is then used to determine the real servo position. The offset is subtracted, the real servo position is filtered to simulate the inertia of the servo and the control valve, and the final position is limited to be between  $0$  and  $32\phi$  mm. If the control valve interlock signal is active, the real servo position is prevented from increasing. The real servo position is then translated to the control valve position by a piece-wise linear function. The valve position is a value between  $0.0$  and  $1.0$  the effective cross sectional area of the control valve is also calculated. The relationship between the position of the control valve and its effective area is nearly linear. Therefore, a linear relationship is assumed. This value is also between  $0.0$  and  $1.0$ .

Finally, the flap valve position is calculated. Its position

is determined by a linear relationship from the pseudo servo position. It is also filtered to account for its inertia. Like the real servo position, the position of the flap valve is not allowed to increase if the control valve interlock signal is active. The flap valve position is also a fractional value.

### 2.3. Testing the Controller Model

The hydraulic turbine controller model was independently subjected to a series of tests to verify that the model adequately simulates the actual controller. In the first of these tests, the setpoint was held constant, and the rotational speed of the turbine was increased. The real servo position and the control valve position both close as is expected. A plot of the results of this test is shown in Figure 6.

The second test involved keeping the rotational speed constant while decreasing the setpoint. In this test, the real servo position and the control valve position also decreased as expected. The results of this test are given in Figure 7. Notice that the flap valve also began to close since the opening of the valve overlaps a little with the opening of the control valve.

In the third test, an increase in power output was simulated. First, the speed decreased as the load increased. This was followed by an increase in the setpoint. Both of these effects cause the control valve to open, to increase the speed back to its nominal value and to increase the power output. The results of this test can be found in Figure 8.

The last test was a simulation of a turbine trip to self consumption. In this situation, the speed increases rapidly as the turbine loses its load. The electro-hydraulic transducer causes the control valve to close quickly to prevent an over-

speed situation. The control valve interlock signal becomes active and remains active until about 25 s after turbine trip. At that time, the valves are allowed to open, and the controller operates the turbine in its no-load state. The plot of the results of this test is given in Figure 9.

These four tests verify the operation of the turbine controller model during normal transients. The results agree quite closely with actual performance data.

#### 2.4. Integrated Testing

Once the turbine controller model had been tested independently, it was integrated into the turbine model for further testing and verification. The last two tests mentioned above /a change of power output and a trip to self consumption/ were repeated with the integrated model. Once again the performance of the simulator models agreed with actual plant data. The results of these two tests can be found in Figures 10 and 11.



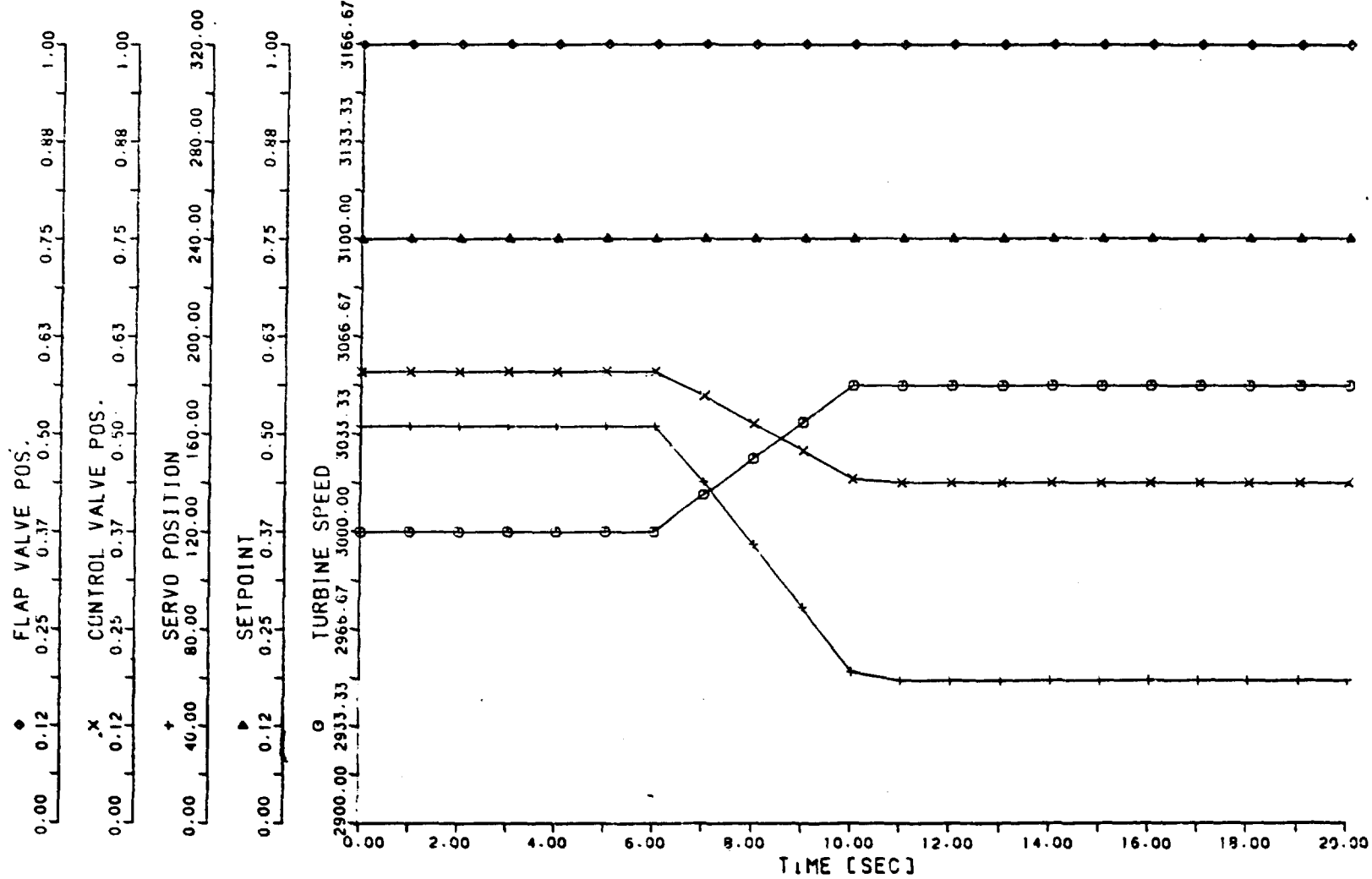


Fig. 6.

STATIC CHARACTERISTICS - CHANGE OF SETPOINT

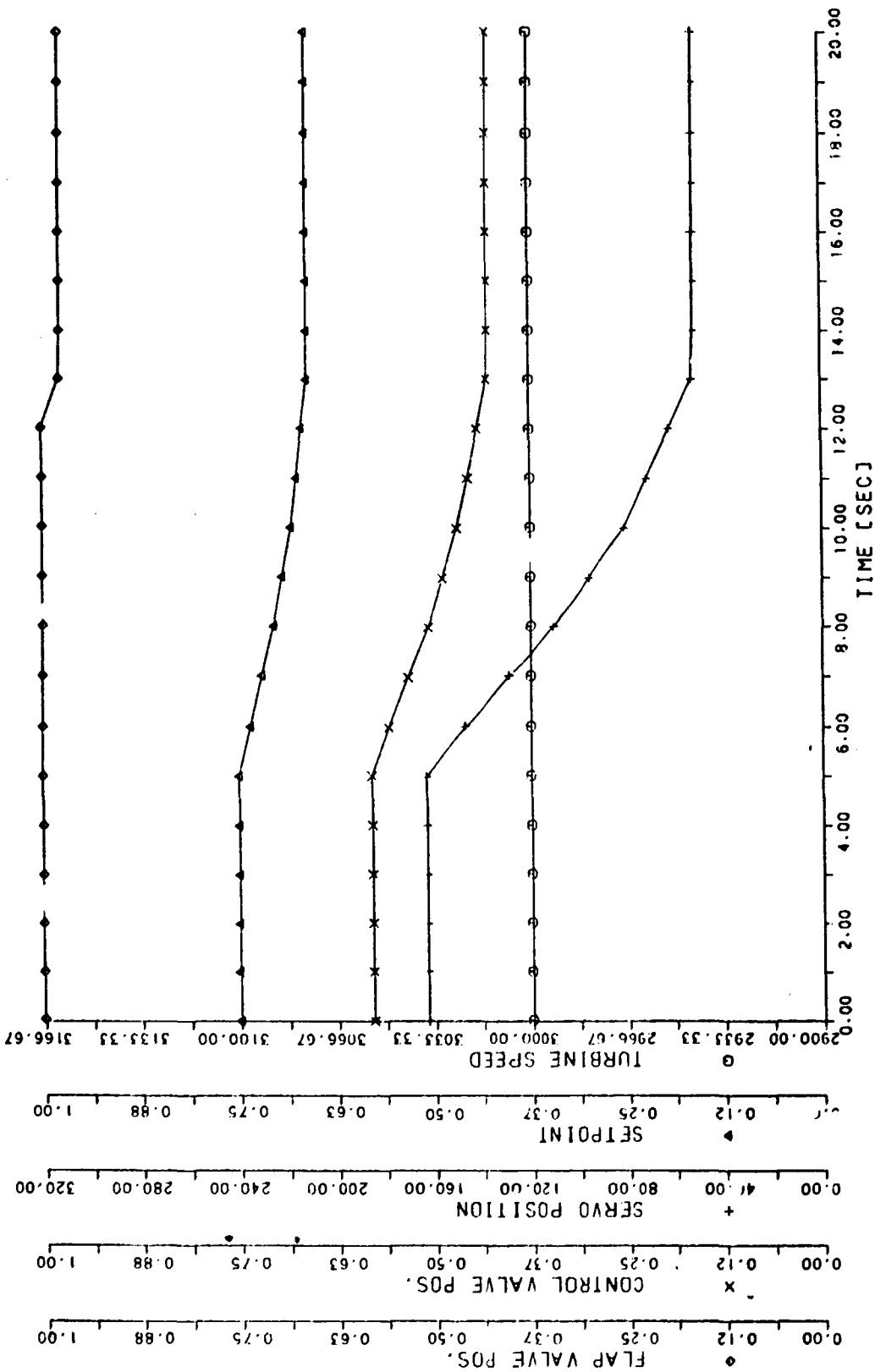


Fig. 7.

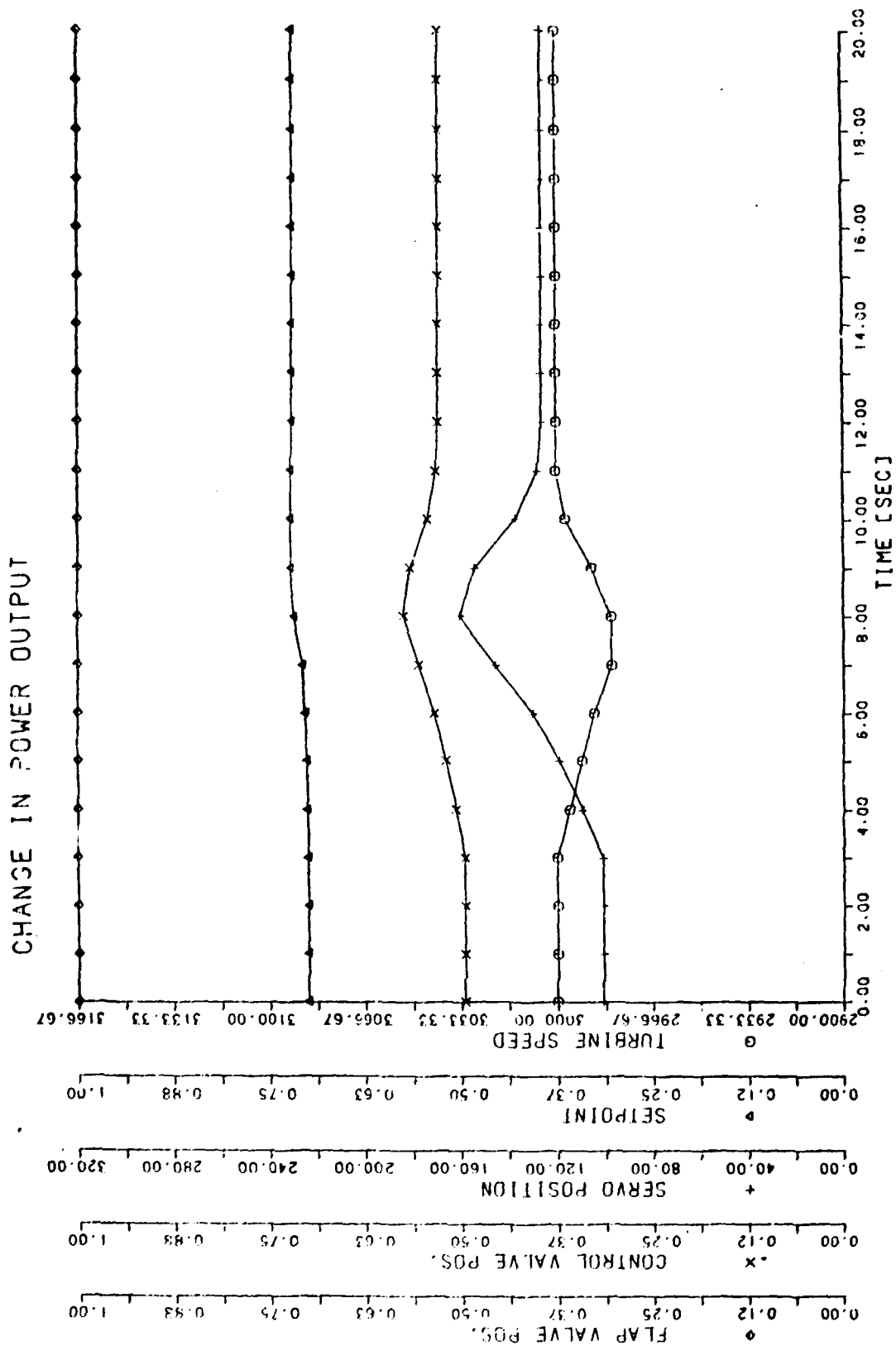


Fig. 8.

TURBINE PROTECTION (TRIP TO SELF-CONSUMPTION)

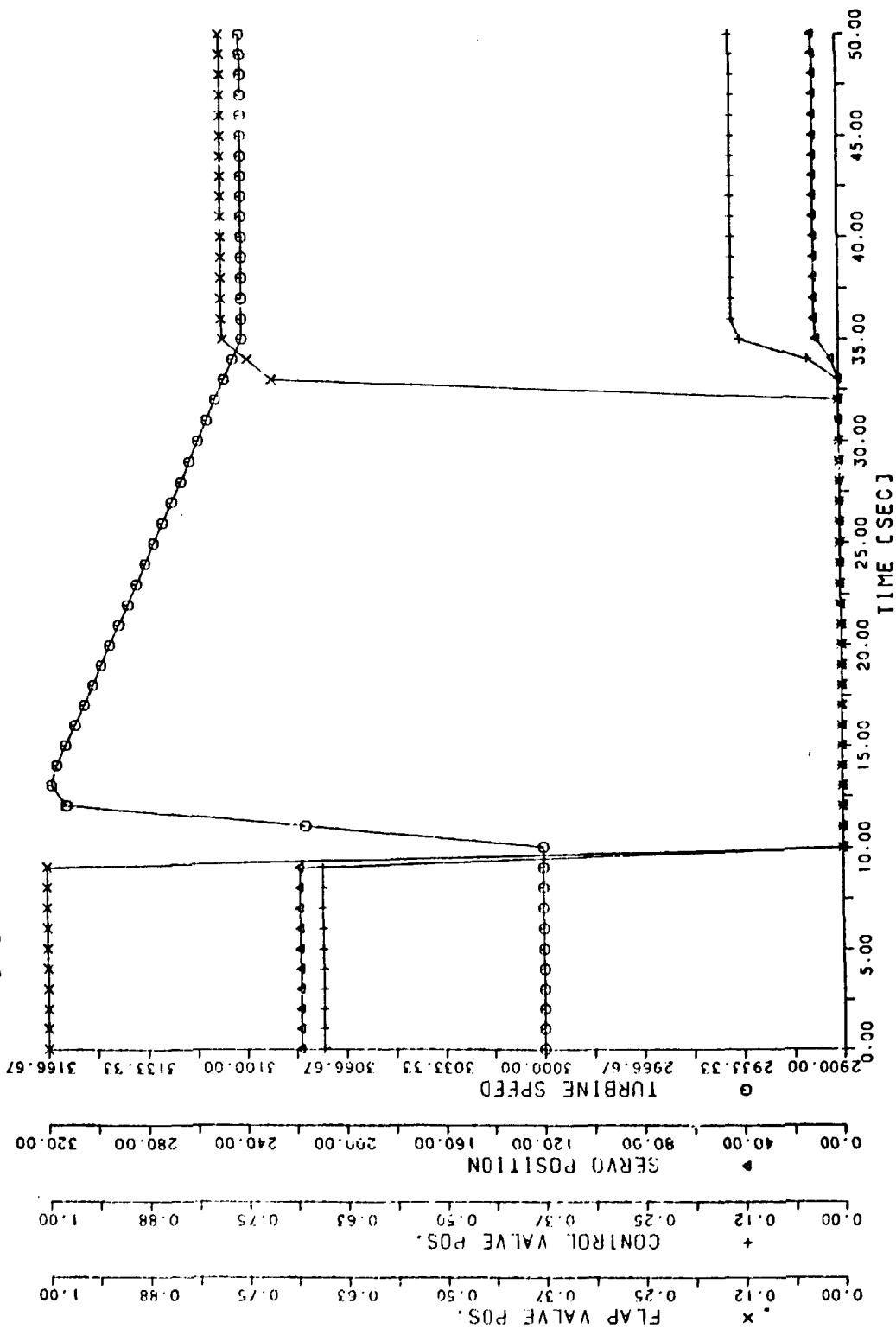


Fig. 9.

CHANGE IN POWER OUTPUT

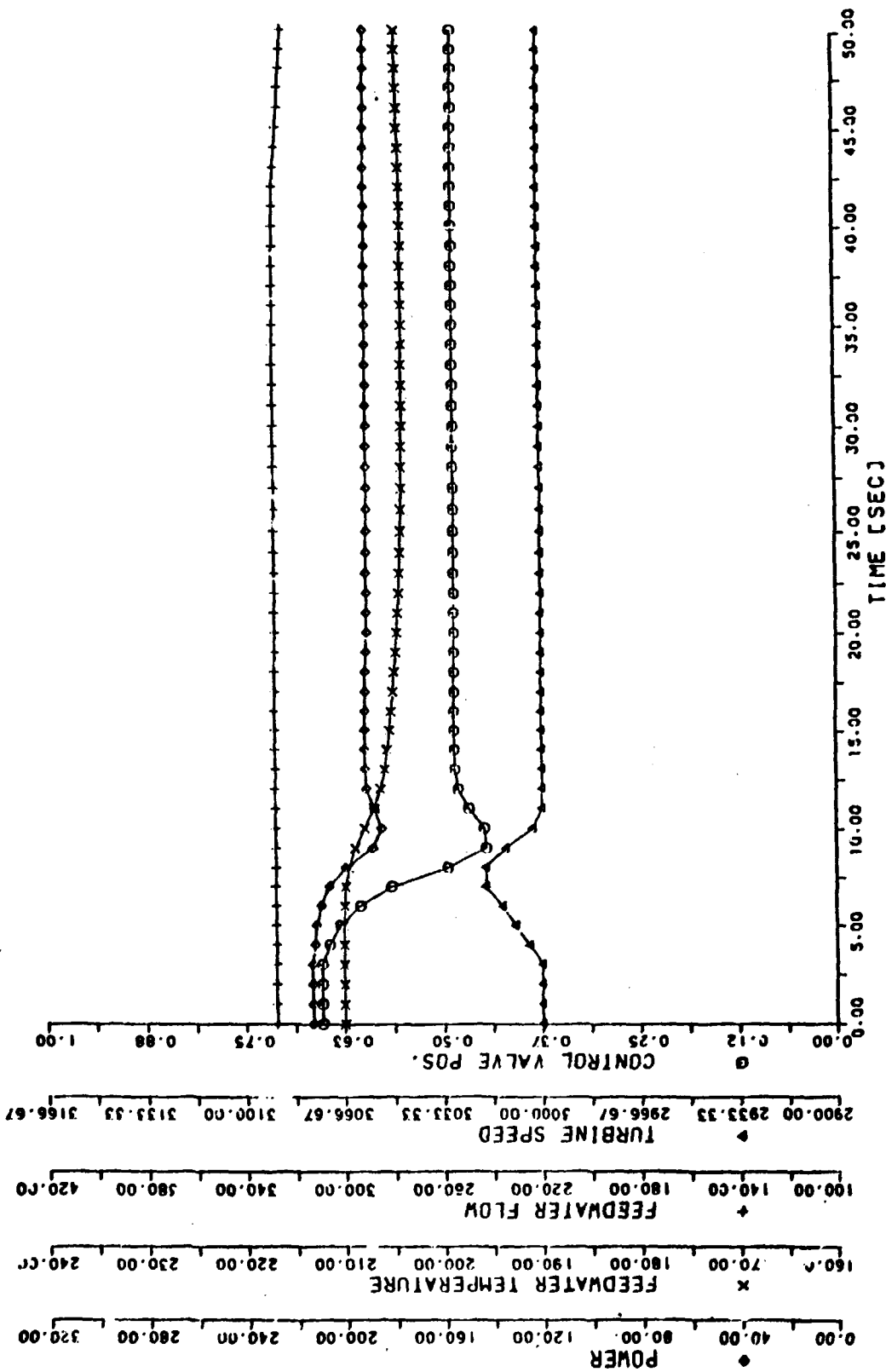


Fig. 10.

TURBINE PROTECTION (TRIP TO SELF-CONSUMPTION)

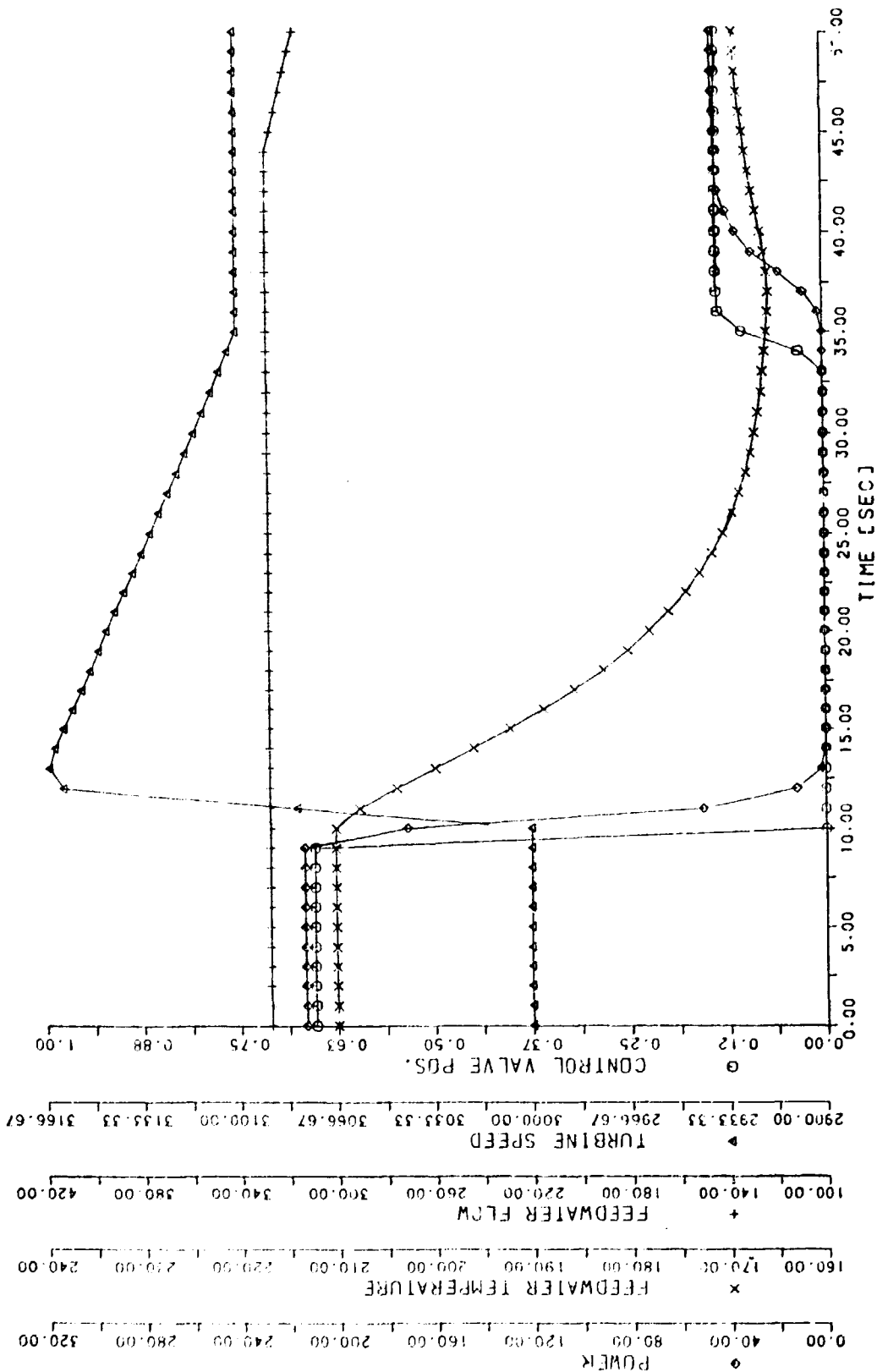
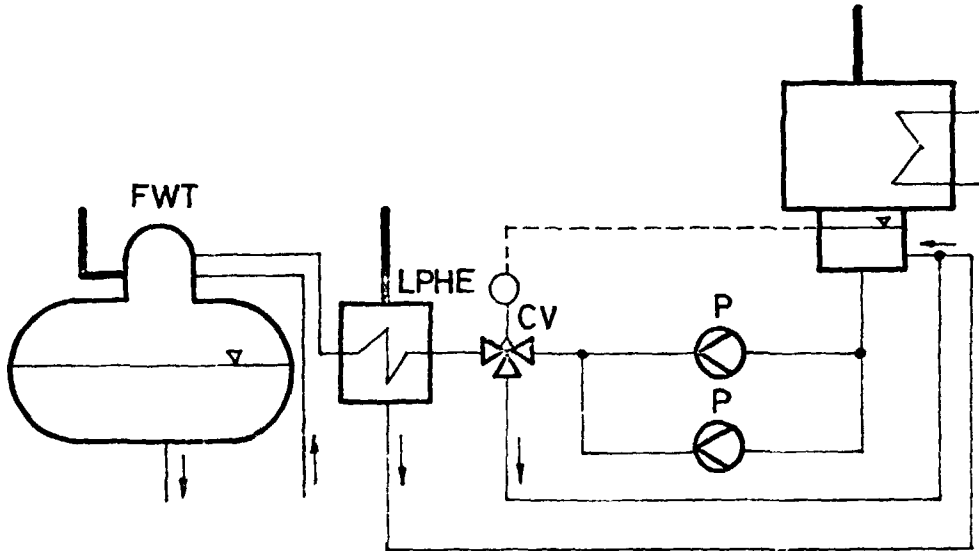


Fig. 11.

### 3. LEVEL CONTROL OF THE CONDENSER HOTWELL

The model of this level controller is illustrated in Figure 11.



- C - condenser hotwell
- P - condensate pump
- CV - three way control valve
- LPHE - low pressure reheater /simplified representation/
- FWT - feedwater tank

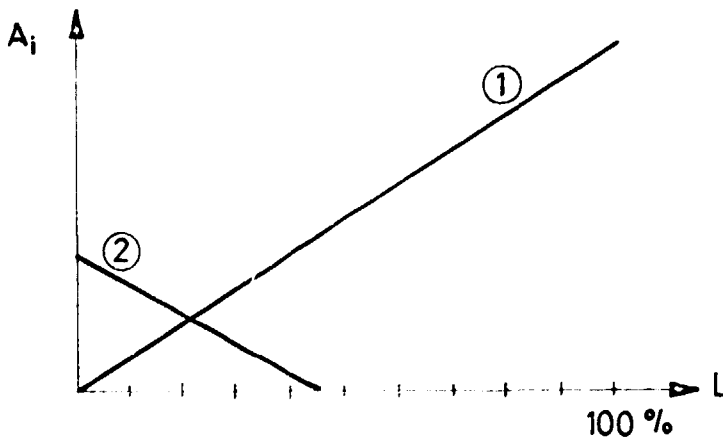
Fig.11

The operation of the controller is as follows: when the level in the condenser hotwell decreases, the control valve moves towards its close position thereby reducing the water flow to the feedwater tank and increasing the recirculation flow back to the condenser hotwell. If on the other hand the level in the hotwell increases, the control valve moves in the open direction which results in a reduction of the recirculation

flow and an increase of water flow into the low pressure reheater and feedwater tank.

For the simulation, some simplifications had to be made:

- the pressure maintained by the pumps should be constant,
- two pumps operate as long as the main steam valve /in front of the turbines/ is open more than 50% of its range, but only one pump operates when the opening of the main steam valve is less than 50%; the starting of the pumps and their trip after they are switched off are not represented in the model,
- the five low pressure reheaters are represented by a simplified model /see Part 1/ and the pressure drop in the reheater depends only on the number of operating pumps,
- the relations of the open cross sections  $A_i$  of the three-way control valve are shown in Figure 12 as a function of valve shaft position  $L$ ,



i=1: open cross section towards the reheater  
i=2: open cross section towards the condenser hotwell  
/recirculation/.

Fig.12



- the flow rate across the control valve is calculated from the open cross section of the valve and the pressure drop in the valve:

$$G = A \sqrt{2 \rho \Delta p} \quad /1/$$

where  $\Delta p$  = the pressure drop,  
 $G$  = the flow rate  
 $A$  = the open cross section  
 $\rho$  = the density of the condensate.

A block diagram of the control algorithm is shown in Figure 13.

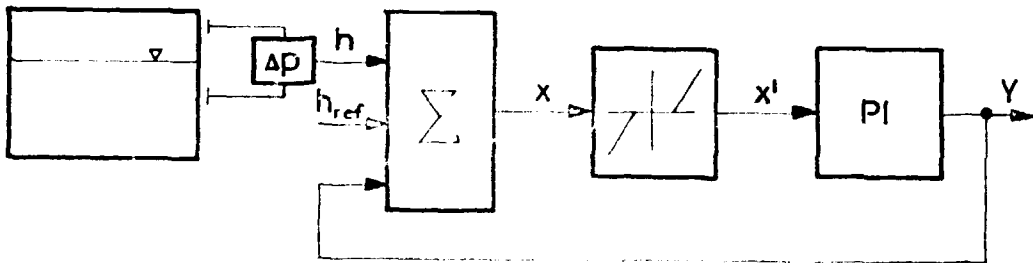


Fig.13

The water level is measured by the pressure-difference of the condenser hotwell. In the simulation model this level is obtained from the mass flow balance in the tank.

Error signal  $x$  is taken as

$$x = C_1 h + C_2 h_{ref} + C_3 \Delta Y \quad /2/$$

where  $h$  = the actual water level

$h_{ref}$  = the nominal water level as the reference signal of the controller,

$\Delta Y$  = the incremental displacement of the control valve

$C_1, C_2, C_3$  = constants determined by measurements.

The input signal to the controller  $X'$  is obtained after taking into account the hysteresis of the system. The controller is an ideal PI /proportional integrating/ controller with the transfer function:

$$Y/S/ = C \left\{ 1 + \frac{1}{sT_I} \right\} X' /S/ \quad /3/$$

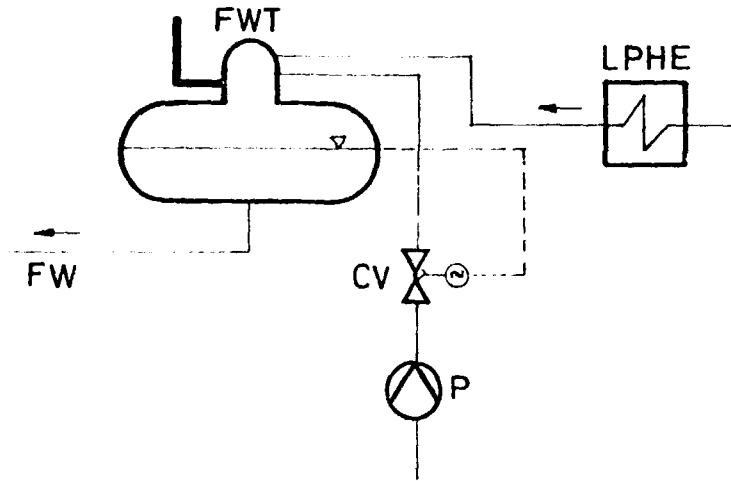
where  $C$  = the proportional coefficient  
 $T_I$  = the time constant of the integration.

The solution of this differential equation gives the  $Y$  position /relative opening compared with nominal opening/ of the control valve.

The speed of the valve position change is limited so that it is constant with realistic valve action times.

#### 4. LEVEL CONTROL OF THE FEEDWATER TANK

The model of the water level controller of the feedwater tank is shown in Figure 14.



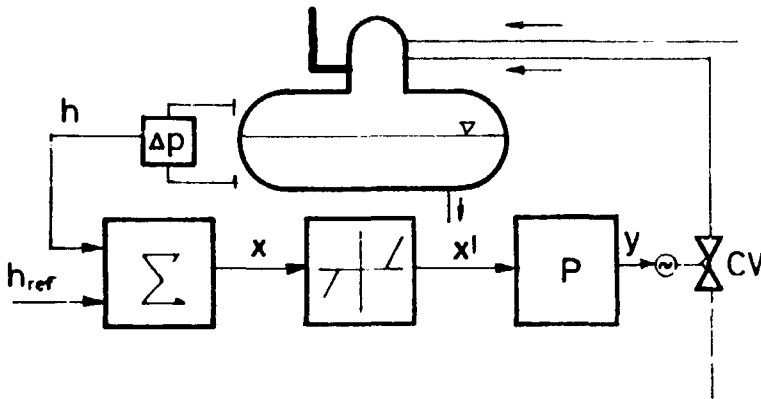
- FW - feedwater
- FWT - feedwater tank
- LPHE - low pressure reheaters  
/simplified representation/
- CV - water level control valve
- P - desalinated water pump

Fig. 14

During the nominal, steady state of the plant, desalinated water is allowed to flow into the secondary circuit to compensate the constant sedimentation losses. This water flows into the feedwater tank through the control valve. The desalination system, however, is not explicitly represented in the simulation, therefore the following assumptions are needed.

The pump supplying the desalinated water line is running continuously at full speed, and a constant pressure is maintained at the inlet of the control valve; similarly, the temperature of the desalinated water is taken as constant.

The block diagram of the algorithm for the feedwater tank water level control is shown in Figure 15.



FWT - feedwater tank  
CV - control valve

Fig.15.

The deviation of the feedwater tank water level from its nominal value is used to calculate the required mass flow from the desalinated water system to the tank that will restore the nominal level in the tank. With pressures known the required mass flow determines the necessary cross section of the valve to be opened. The valve characteristic that gives the open cross section as a function of valve shaft position is simply obtained.

The mass flow rate of the desalinated water into the feedwater tank is finally modified by taking into account the limitation due to the realistic valve speed.

The issues of the KFKI preprint/report series are classified as follows:

- |   |  |
|---|--|
| A. Particle and Nuclear Physics                           | H. Laboratory, Biomedical and Nuclear Reactor Electronics                |
| B. General Relativity and Gravitation                     | I. Mechanical, Precision Mechanical and Nuclear Engineering              |
| C. Cosmic Rays and Space Research                         | J. Analytical and Physical Chemistry                                     |
| D. Fusion and Plasma Physics                              | K. Health Physics  |
| E. Solid State Physics                                    | L. Vibration Analysis, CAD, CAM  |
| F. Semiconductor and Bubble Memory Physics and Technology | M. Hardware and Software Development, Computer Applications, Programming |
| G. Nuclear Reactor Physics and Technology                 | N. Computer Design, CAMAC, Computer Controlled Measurements              |

The complete series or issues discussing one or more of the subjects can be ordered; institutions are kindly requested to contact the KFKI Library, individuals the authors.

Title and classification of the issues published this year:

- |   |  |
|---|--|
| KFKI-1987-01/A<br>V.Sh. Gogokhia et al. | Nonperturbative approach to quark propagator in the covariant, transverse gauge  |
| KFKI-1987-02/M<br>M. Barbuceanu et al.  | Integrating declarative knowledge programming styles and tools for building expert systems   |
| KFKI-1987-03/G<br>L. Szabados et al.    | Primary loop dynamical investigations. Part 1. Computerized analysis of the total loss of flow in the Paks NPP on the basis of PMK-NVH experimental data /in Hungarian/                  |
| KFKI-1987-04/G<br>Gy. Egely             | Critical comparison of nuclear safety reports. Part 1. Practice followed in the USA and in FRG /in Hungarian/  |
| KFKI-1987-05/G<br>Gy. Ézsöli et al.     | A 7.4% cold leg break without SIPs. Description of the measurement /in Hungarian/  |
| KFKI-1987-06/G<br>Gy. Ézsöli et al.     | Primary loop dynamical investigations. Part 1. Experimental investigation of the total loss of flow in the Paks NPP in the PMK-NVH facility /in Hungarian/                               |
| KFKI-1987-07/G<br>L. Szabados et al.    | A calculation method for the operation of the Paks NPP based on the subchannel approach. Part 1. A computing procedure and method applicable as part of the VERONA system /in Hungarian/ |
| KFKI-1987-08/B<br>L.B. Szabados         | Commutation properties of cyclic and null Killing symmetries   |
| KFKI-1987-09/E<br>G. Györgyi et al.     | Relaxation processes in chaotic states of one dimensional maps   |
| KFKI-1987-10/D<br>Gy. Egely             | Hungarian ball lightning observations (case 1 - case 278)  |

KFKI-1987-11/M H. König	Developing protocol test software using the PDL-system
KFKI-1987-12/M D. Nicholson et al.	Advanced help through plan instantiation and dynamic partner modelling
KFKI-1987-13/M Katalin Tarnay et al.	Experiments with a network environment manipulator /in Hungarian/
KFKI-1987-14/A H.W. Barz et al.	Deconfinement transition in anisotropic matter
KFKI-1987-15/M R. Wittmann	An algebraic specification method for describing the protocols of computer networks /in Hungarian/
KFKI-1987-16/G O. Aguilar et al.	Monitoring temperature reactivity coefficient by noise method in a NPP at full power
KFKI-1987-17/M G. Németh et al.	Collection of scientific papers in collaboration with Joint Institute for Nuclear Research, Dubna, USSR and Central Research Institute for Physics, Budapest, Hungary. Algorithms and programs for solution of some problems in physics. Fifth volume
KFKI-1987-18/E G. Egely et al.	Experimental investigation of biologically induced magnetic anomalies
KFKI-1987-19/A B. Milek et al.	A model for particle emission from a fissioning system
KFKI-1987-20/M S. Wagner-Dibuz	The specification and testing of transport protocols /in Hungarian/
KFKI-1987-21/E B. Lukács et al.	Elementary quantum physical description of triplet superconductors
KFKI-1987-22/G M. Makai et al.	DIGA/NSL - New calculational model in slab geometry
KFKI-1987-23/A J. Erő et al.	Production of protons, deuterons and tritons on carbon by intermediate energy neutrons
KFKI-1987-24/K I. Balásházy et. al	Gamma-spectrometric examination of hot particles emitted during the Chernobyl accident
KFKI-1987-25/K A. Andrásí et al.	Application of Ge-spectrometry for rapid in-situ determination of environmental radioactivity
KFKI-1987-26/G J. Végh	Neutron spectrum measurement in the channel No. 182/5 of the KFKI WWR-SM reactor
KFKI-1987-27/A S. Krasznovszky et al.	Universal description of inelastic and non(single)-diffractive multiplicity distributions in pp collisions at 250, 360 and 800 GeV/c
KFKI-1987-28/M F. Adorján et al.	VERONA-plus extended core-monitoring system for WWER-440 type nuclear power plants
KFKI-1987-29/G J. Végh et al.	Application of boron filters for neutron spectrum determination purposes in various neutron environments
KFKI-1987-30/E N. Menyhárd	Inhomogeneous mean field approximation for phase transitions in probabilistic cellular automata - An example

KFKI-1987-31/M G. Németh et al.	Computation of generalized Padé approximants
KFKI-1987-32/E I. Pócsik	Lone-pair model for high temperature superconductivity
KFKI-1987-33/B L.B. Szabados	Causal boundary for strongly causal space-time
KFKI-1987-34/A Z. Fodor et al.	Proton detection efficiency of a plastic scintillator telescope
KFKI-1987-35/C R.Z. Sagdeev et al.	Near nuclear region of comet Halley based on the imaging results of the VEGA mission
KFKI-1987-36/E Gy. Szabó	Thermodynamic aspects of chemically curved crystals
KFKI-1987-37/A T. Nagy et al.	Lepton + lepton + photon decays and lepton g-2 factors in gauge theories
KFKI-1987-38/K S. Deme et al.	Real-time computing in environmental monitoring of a nuclear power plant
KFKI-1987-39/K L. Koblinger	A review of Monte Carlo techniques used in various fields of radiation protection
KFKI-1987-40/A J. Balog et al.	Lattice classification of the four-dimensional heterotic strings
KFKI-1987-41/E I. Furó et al.	Evidence of antiferromagnetic ordering in $\text{La}_2\text{CuO}_4$ re-interpretation of $^{139}\text{La}$ nuclear quadrupole resonance (NQR) data
KFKI-1987-42/J Á. Vértes et al.	Kinetic energy distribution of ions generated by laser ionization sources
KFKI-1987-43/E Z. Juhász	Variations of the transfer function during $\text{Bi}_4\text{Ge}_3\text{O}_{12}$ growth
KFKI-1987-44/G A. Gács et al.	Simulation of the dynamic behaviour of the secondary circuit of a WWER-440 type Nuclear Power Plant
KFKI-1987-45/M,N H. Koenig et al.	An intelligent protocol workstation
KFKI-1987-46/M,N P. Ecsedi Tóth et al.	Formal description oriented performance evaluation of protocols
KFKI-1987-47/A N.P. Aleshin et al.	Study of proton-deuteron break-up reaction in exclusive experiment at 1 GeV
KFKI-1987-48/E B. Sas et al.	Scattering mechanisms and transport properties of FeTM3 amorphous alloys
KFKI-1987-49/E A.G. Balogh et al.	Positron annihilation study on Y-Ba-Cu-O high $T_c$ superconductors
KFKI-1987-50/C R.Z. Sagdeev et al.	Plasma phenomena around comets: interaction with the solar wind
KFKI-1987-51/D D. Hildebrandt et al.	Impurity injection into tokamak plasmas by erosion probes
KFKI-1987-52/A J. Zimányi et al.	An interpretable family of equations of state for dense hadronic matter

KFKI-1987-53/G L. Bürger et al.	Real-time executive for a basic principle simulator
KFKI-1987-54/E G. Konczos et al.	Recent progress in the application of soft magnetic amorphous materials: alloys, preparation, devices
KFKI-1987-55/E Nguyen Minh Khue	A Green's function treatment of giant polariton problem in molecular semiconductors
KFKI-1987-56/G Gy. Ézsöl et al.	7.4% cold leg break with SITs and HPIS in action /in Hungarian/
KFKI-1987-57/C Z. Bazsó et al.	7.4% cold leg break without SITs and HPIS in action /in Hungarian/
KFKI-1987-58/G Tran Quoc Dung et al.	DUMA - a program to display distributions in hexagonal geometry
KFKI-1987-59/G S. Mikó et al.	Method for determining outlet temperature of fuel assemblies in the VVER-440 core, which are not furnished with direct temperature measurement /in Hungarian/
KFKI-1987-60/A T. Dolinszky	Strong coupling expansions for repulsive cut-off potentials
KFKI-1987-61/P M. Füstöss-Wégnér et al.	Effect of microinhomogeneities on collection efficiency spectra in (p-i-n) a-Si:H junctions
KFKI-1987-62/D J.S. Bakos	Gas laser research in Hungary
KFKI-1987-63/B L. Fülöp	The harmonic oscillator in the forceless mechanics of Hertz and in the Riemannian space-time geometry
KFKI-1987-64/J Á.G. Nagy et al.	Steric interactions of ferrocenyl ketones: A comparative evaluation of data from <sup>13</sup> C NMR and IR spectroscopy and cyclical voltammetry /in Hungarian/
KFKI-1987-65/G,J H. Illy	Recent bibliography on analytical and sampling problems of a PWK primary coolant Supplement V.
KFKI-1987-66/D,E,F M.A. Algatti et al.	Experimental investigations on nonequilibrium electron and thermal light emission from metals induced by short laser pulses
KFKI-1987-67/G,M J. Gadó et al.	WWER-1000 core physical model /in Hungarian/
KFKI-1987-68/G,M L. Maróti et al.	WWER-1000 core thermohydraulic model /in Hungarian/
KFKI-1987-69/G,M M. Fodor et al.	Fuel behaviour /in Hungarian/
KFKI-1987-70/E L. Bata et al.	Measurement of spontaneous polarization of smectics C doped with a chiral additive
KFKI-1987-71/A A. Margaritis et al.	Series expansion solution of the Wegner-Houghton renormalisation group equation
KFKI-1987-72/G L. Perneczky et al.	Assessment of possible accident scenarios. Analysis of the loss of feedwater transient. /in Hungarian/



KFKI-1987-73/G L. Szabados et al.	Investigation of the loss of feedwater transient on the PMK-NVH test facility. Test evaluation and computer code analysis /in Hungarian/
KFKI-1987-74/B B. Lukács	Neutron stars with orbiting light?
KFKI-1987-75/C R.Z. Sagdeev et al.	The rotation of P/Halley
KFKI-1987-76/G L. Szabados et al	The hot channel operation method for the Paks NPP. Part. II. Theoretical and experimental investigation of transient process initiated by the blockage of the rotor of pump /in Hungarian/
KFKI-1987-77/B I. Rácz	Causal boundary for stably causal space-times
KFKI-1987-78/E K. Tompa	Accelerator produced beta-active nuclei in materials science
KFKI-1987-79/E L. Rosta et al.	Multidisc neutron velocity selector
KFKI-1987-80/A T. Dolinszky	Extension of the Born series fully off the energy shell
KFKI-1987-81/G J. Doorentos et al.	Simulation of the dynamic behaviour of the secondary circuit of a WWER-440 type Nuclear Power Plant. Part 2

Kiadja a Központi Fizikai Kutató Intézet  
Felelős kiadó: Gyimesi Zoltán  
Szakmai lektor: Perneczky László  
Nyelvi lektor: Harvey Shenker  
Példányszám: 224 Törzsszám: 87-571  
Készült a KFKI sokszorosító üzemében  
Felelős vezető: Tőrekői Béláné  
Budapest, 1987. december hó